

Universal features of counting statistics of thermal and quantum phase slips in superconducting nanocircuits

A. Murphy,¹ P. Weinberg,² T. Aref,^{1,*} U.C. Coskun,¹ V. Vakaryuk,³ A. Levchenko,² and A. Bezryadin¹

¹*Department of Physics, University of Illinois at Urbana-Champaign, Urbana, Illinois 61801, USA*

²*Department of Physics and Astronomy, Michigan State University, East Lansing, Michigan 48824, USA*

³*Institute for Quantum Matter and Department of Physics & Astronomy,*

The Johns Hopkins University, Baltimore, Maryland 21218, USA

(Dated: May 21, 2013)

We perform measurements of phase-slip-induced switching current events on different types of superconducting weak links and systematically study statistical properties of the switching current distributions. We employ two types of devices in which a weak link is formed either by a superconducting nanowire or by a graphene flake subject to proximity effect. We demonstrate that, independently on the nature of the weak link, higher moments of the distribution take universal values. In particular, the third moment (skewness) of the distribution is close to -1 both in thermal and quantum regimes. The fourth moment (kurtosis) also takes a universal value close to 5. The discovered universality of skewness and kurtosis is confirmed by an analytical model. Our numerical analysis shows that introduction of extraneous noise into the system leads to significant deviations from the universal values. We suggest to use the discovered universality of higher moments as a robust tool for checking against undesirable effects on noise in various types of measurements.

PACS numbers: 74.78.Na, 74.50.+r, 74.25.Sv, 74.40.-n

Introduction.—The field of quantum noise has recently seen rapid development caused both by its growing significance in many areas of condensed matter physics as well as by a constant improvement in the capabilities of high precision measurements [1]. Perhaps the most intensively studied question to date is related to the statistics of charge transport in mesoscopic conductors. In such systems probability distribution of current fluctuations, the so-called full counting statistics, was rigorously derived for various normal and superconducting circuits [2] and tested in the state-of-the-art measurements of the third moment (skewness) of current fluctuations [3]. Given that charge is a quantum mechanical conjugate variable to the phase, it is of fundamental interest to study corresponding statistics of phase fluctuations. Superconducting nanowires and related proximity devices offer a natural platform for this purpose, which we explore in the present work.

The macroscopic quantum tunneling of the phase across a current-biased Josephson junction [4] or a superconducting nanowire [5–7] is arguably the most profound and well-known manifestation of quantum fluctuations at the macroscopic level. This phenomenon is observed by registering phase slip events [8], which proliferate at currents close to the critical and drive transitions between supercurrent-carrying and dissipative branches of current-voltage characteristics [6, 7, 9, 10]. Macroscopic quantum tunneling is usually described in the framework that treats quantum or thermally activated transitions of the phase between neighboring minima of a tilted washboard potential in the presence of a dissipative environment [4, 5, 11]. Complimentary approaches employ an effective action for BCS superconductors [9, 10, 16].

Unlike experiments associated with the charge transfer where measurements of each moment of the full counting statistics is beyond current experimental capabilities, experiments on switching current allow one to reconstruct full distribution of superconducting phase fluctuations since a single phase slip is sufficient to drive the system into resistive state [7, 17] by creating a hot spot [18, 19]. Thus there exists a one-to-one correspondence between phase fluctuations - *phase slips* - and switching events.

In this Letter we report a systematic study of higher moments of the switching current distribution as a function of temperature and other parameters of our devices. The higher moments under investigation include skewness S that quantifies an asymmetry of the distribution, and kurtosis K that is a measure of its peakedness (for definitions see below). We present evidence, both experimental and theoretical, that these higher moments are in fact universal constants: $S \approx -1$ and $K \approx 5$. Surprisingly, the observed crossover from a classical escape mechanism (i.e., the thermal activation) to a quantum one (i.e., quantum tunneling from a metastable energy minimum) does not lead to any noticeable changes in these moments. We evince this universality using two types of samples, namely graphene junctions under the proximity effect as well as ultra-thin superconducting nanowires. Apparent universality of S and K has to be contrasted with the behavior of the standard deviation of the switching current (the second moment σ) that exhibits nontrivial temperature dependence: the power-law [20], $\sigma \propto T^{2/3}$, in the thermal regime and $\sigma \propto \text{const}$ in the quantum regime [7, 9, 10, 17].

Devices.—Nanowire samples were prepared [10, 21] by depositing carbon nanotubes across a 100 nm wide trench

on a silicon chip, coated by a film of SiO_2 and a film of SiN . A film of 10-20nm of $\text{Mo}_{76}\text{Ge}_{24}$ was sputtered onto the chip, covering the top SiN surface and the nanotubes crossing the trench. Thus the suspended segments of nanotubes were converted into nanowires. Uniform wires were selected using SEM, and the MoGe film was patterned by photolithography, to define contact pads (electrodes). In such devices the selected nanowire serves as the only conducting link connecting the superconducting thin-film electrodes, positioned on the opposite sides of the trench. Importantly, there is no additional contact resistance between the nanowire and the contact pad since the wire transforms seamlessly into the pad while both are made in the same sputtering run.

Graphene flakes were deposited onto SiO_2 surface by mechanical exfoliation [22]. Electron-beam lithography was utilized to pattern the electrodes into a comb shape. After the resist was exposed and developed, we deposit, using thermal evaporation, a 4 nm Pd film (so-called sticking layer) and a 100 nm Pb film on the top. Lift-off was performed by placing the sample in an acetone bath for five minutes, sonicating it for ten seconds every other minute. The 100nm Pb layer induces superconductivity in the graphene through the proximity effect. The samples were measured in a He-3 cryostat. Electromagnetic noise was filtered from the system using π -filters at room temperature and a copper powder and silver-paste radio-frequency noise filters at low temperatures.

A sinusoidal bias current, having an amplitude greater than the critical current of the device, was applied across each sample. As the current increased from zero to its maximum, the voltage across the sample demonstrated a sudden jump from zero to some large, non-zero value, indicating the system switched from a superconducting state to a normal, resistive state. The value of bias current at which the jump took place was recorded as the switching current. Then the bias current returned to zero, and the system once again became superconducting. This process was repeated $N = 10^4$ times (or 5000 in some cases) for each set of parameters. Each measurement gave slightly different value of the switching current, due to inherent stochasticity of the phase slips, thus producing switching current distributions. The skewness and kurtosis of each distribution was calculated from the recorded data by using standard expressions: $S = N^{-1} \sum_{i=1}^N (I_{sw,i} - \langle I_{sw} \rangle)^3 / \sigma^3$ and $K = N^{-1} \sum_{i=1}^N (I_{sw,i} - \langle I_{sw} \rangle)^4 / \sigma^4$, where each $I_{sw,i}$ represents an applied bias current at which a switching event took place, $\langle I_{sw} \rangle$ is the mean switching current, and σ is the standard deviation of the switching distribution.

Experimental results.—We first discuss the effect of temperature on the skewness and kurtosis of the switching current distributions. We find that in both types of

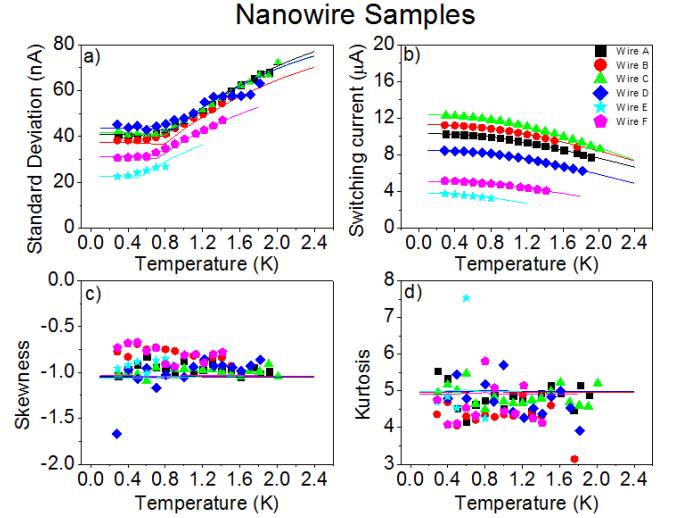


FIG. 1: (a) standard deviation, (b) mean switching current, (c) skewness, and (d) kurtosis of the switching current distributions in nanowire samples A, B, C, D, E and F vs temperature T . The experimental values are represented by symbols. Simulation curves are shown by solid lines. One point in figure (c) and two points in figure (d) lie outside the ranges shown. Fitting parameters used in the simulation are summarized in Table I of the Supplementary Material [23].

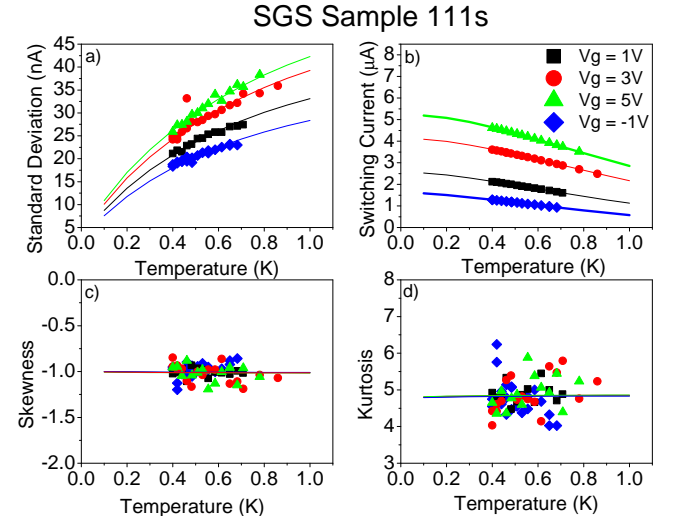


FIG. 2: (a) standard deviation, (b) mean switching current, (c) skewness, and (d) kurtosis of the switching current distributions in SGS sample 111s vs temperature at a gate voltages of 1V, 3V, 5V and -1V. We use the same convention as in the previous figure. One point in figure (c) lies outside the range shown. Fitting parameters used in the simulation are summarized in Table II of the Supplementary Material [23]. Data for SGS sample 105s are shown in [23].

samples – superconducting nanowires (Figs. 1c-1d), and graphene proximity junctions (Figs. 2c-2d) – the skewness and kurtosis are constant with temperature. Surprisingly, these moments are identical within experimental uncertainty for the two qualitatively different systems.

The value of the skewness in both cases is near -1 , and the value of kurtosis is near 5 . In nanowire samples, these moments remain constant even as the system experiences a crossover from the high temperature regime, at which phase slips are predominantly caused by thermally activation, to low temperatures, at which quantum tunneling of phase slips is responsible for the premature switching. This crossover is evident in Fig. 1a as the standard deviation changes from the power-law at high temperatures to a constant value at low temperatures. The classical-to-quantum crossover temperature is typically in the range $0.6\text{--}0.8$ K for the studied samples (Fig. 1).

In SGS samples in addition to the temperature dependence we also study the effect of gate voltage V_g on the skewness and kurtosis. Both moments remain constant within the experimental uncertainty over a wide range of T and V_g (see Figs. 2c-d and [23]). It should be noted that, unlike nanowire samples, SGS junctions do not show crossover to the quantum tunneling dominated regime within experimentally tested temperatures. However, we do expect that such crossover might occur at lower temperatures, as recently reported [24].

We also demonstrate numerically [23], that the presence of extraneous noise leads to a substantial reduction of the universal moments. This observation provides an independent tool for assessing the relevance of noise to the interpretation of experimental data.

Numerical simulations and fitting.— The fitting curves presented in Figs. 1 and 2 were obtained using the Arrhenius-type activation formula for the rate of phase slips (hereafter $\hbar = k_B = 1$) [10, 25]

$$\Gamma(I, T) = \Omega(I, T) \left[e^{-U(I, T)/T} + e^{-U(I, T)/T_q} \right], \quad (1)$$

which accounts for both thermal and quantum escape processes. Here Ω is the attempt frequency, U is the energy barrier for a phase slip, T is the base temperature and T_q is the quantum temperature used to model the regime of macroscopic quantum tunneling observed in nanowire samples at low temperatures [26]. For both systems activation energy has power-law functional dependence on the applied bias current

$$U(I, T) = \frac{\kappa I_c(T)}{e} (1 - I/I_c(T))^\eta. \quad (2)$$

For SGS devices we took $\kappa = \sqrt{8}/3$ and $\eta = 3/2$ [27, 28] and used a critical current in the form

$$I_c(T) = \frac{64\pi T}{eR_N} \sum_{n=0}^{\infty} \frac{\Delta^2(L/L_n) \exp(-L/L_n)}{[\omega_n + W_n + \sqrt{2(W_n^2 + \omega_n W_n)}]^2} \quad (3)$$

where R_N is the normal state resistance of a junction, Δ is the superconducting gap in the leads, $\omega_n = (2n+1)\pi T$, $W_n = \sqrt{\Delta^2 + \omega_n^2}$, $L_n = \sqrt{D/2\omega_n}$. The sum over n was taken until convergence (roughly 10 terms). Expression (3) follows from the theory of disordered superconductor-normal metal-superconductor junctions [29–31]. It has to

be stressed that ballistic theory of the proximity effect in SGS junctions [32] fails to account for the temperature and gate voltage dependencies of the critical current for our devices (see Fig. 2b). This observation is also consistent with the previous reports on the proximity effect in SGS systems [24, 27, 33–38]. From the normal state resistance of our samples, we deduce typical mean free path $l \sim 20\text{nm}$, which correspond to the diffusion coefficient $D \sim 50\text{cm}^2/\text{s}$. Because the mean free path and the Thouless energy $E_{Th} = D/L^2 \sim 80\mu\text{eV}$ are much smaller than the junction spacing of $L \sim 300\text{nm}$ and the energy gap $\Delta \sim 1\text{meV}$, respectively, our SGS junctions correspond to a long diffusive junction limit.

For superconducting nanowires there are two known models for U in Eq. (2). If a wire forms a phase slip junction (PSJ) then $\kappa = \sqrt{6}/2$ and $\eta = 5/4$ [1, 2, 8, 9]. The corresponding expressions for κ and η for the more thoroughly studied case of a Josephson junction have the same values as above for the SGS devices. It is worth noting that qualitatively the two models are very similar. Following the previous work [42] we model the critical current of nanowire devices by the phenomenological Bardeen's formula [43]

$$I_c(T) = I_c(0)(1 - T^2/T_c^2)^{3/2}. \quad (4)$$

Finally, for both SGS and nanowire systems the escape attempt frequency in Eq. (1) was described by

$$\Omega(I, T) = \Omega_0(T)(1 - I/I_c(T))^\nu \quad (5)$$

with $\nu = 1/4$ for JJ model, and $\nu = 5/8$ for PSJ model.

Eqns. (1)–(5) were combined to determine the rate of phase slips. For a given set of parameters this rate was used to predict the switching distribution as a function of bias current and then calculate its mean, standard deviation, skewness and kurtosis. Such procedure was repeated at different temperatures to produce the temperature dependence of the moments. In the case of SGS samples the above scheme was also repeated at different gate voltages. Parameters (Ω_0 , $I_c(0)$, T_c , T_q) for nanowire samples and (Ω_0 , R_N , T_c and D) for SGS samples were then adjusted within the expected range of values until the predicted switching current and standard deviation vs temperature curves matched the data. These, along with the resulting skewness and kurtosis curves were used as fits to the data and are plotted as solid lines in Figs. 1 and 2 [23, 44].

Analytical model.— In this section we compute skewness and kurtosis by using an approach developed for the problem of escape from a metastable potential well subject to a steadily increasing bias field [20, 45]. We consider a general situation in which the phase slip rate of the system – either thermal or quantum – can be written in terms of the reduced current variable $\epsilon = 1 - I/I_c$ as

$$\Gamma(\epsilon) = A\epsilon^{a+b-1} \exp(-B\epsilon^b). \quad (6)$$

This form is general enough to cover all range of parameters relevant for our experiment on both types of devices. The powers a and b depend on whether the escape is quantum or thermally activated, while parameters A and B depend on the degree and type of damping (in particular, we estimate that our SGS junctions are moderately underdamped with the quality factor $Q \simeq 4$). The distribution function for phase slips can be expressed in terms of the rate as

$$P(\epsilon) = \frac{1}{|\dot{\epsilon}|} \Gamma(\epsilon) \exp \left[-\frac{1}{|\dot{\epsilon}|} \int_{\epsilon}^{\infty} \Gamma(\epsilon') d\epsilon' \right] \quad (7)$$

where $|\dot{\epsilon}|$ is a constant ramp speed. We are interested in central moments m_n of variable ϵ i.e. moments defined around its mean value $\bar{\epsilon}$:

$$m_n \equiv \langle (\epsilon - \bar{\epsilon})^n \rangle = \int_0^{\infty} d\epsilon (\epsilon - \bar{\epsilon})^n P(\epsilon) \quad (8)$$

where $\bar{\epsilon} = \int_0^{\infty} d\epsilon \epsilon P(\epsilon)$. Dispersion, skewness and kurtosis can be expressed in terms of central moments. To this end, it is convenient to introduce a dimensionless parameter

$$Z = \ln \left[\frac{A/|\dot{\epsilon}|}{bB^{1+a/b}} \right], \quad (9)$$

which only weakly depends on the characteristics of the system in question. For self-consistency of the description this parameter should be large which can be achieved by tuning the ramp speed $|\dot{\epsilon}|$.

It is straightforward to show that moments of distribution (7) can be written as an asymptotic power series in $1/Z \ll 1$ as follows:

$$\langle \epsilon^n \rangle = B^{-n/b} Z^{n/b} \left[1 + \sum_{j=1} Z^{-j} f_j(n, \ln Z) \right]. \quad (10)$$

Definition of the expansion coefficients f_j are relegated to the Supplementary Material [23] because of their cumbersome form. Within the model f_j depend on power exponents a and b , and very weakly (as a double logarithm), on temperature-dependent parameters A and B , and the ramp speed $|\dot{\epsilon}|$. This implies that temperature scaling of both moments $\langle \epsilon^n \rangle$ and central moments $\langle (\epsilon - \bar{\epsilon})^n \rangle$ is fully dominated by the temperature scaling of B which is proportional to the height of the phase slip barrier $\{\langle \epsilon^n \rangle, \langle (\epsilon - \bar{\epsilon})^n \rangle\} \propto B^{-n/b}(T)$. To determine proportionality coefficients one needs to use the explicit form of f_j . Up to the order $1/Z$ first two moments are given by

$$\bar{\epsilon} = Z^{1/b} B^{-1/b} \left(1 + \frac{v/b}{Z} \right), \quad (11)$$

$$\sigma^2 \equiv m_2 = Z^{2/b-2} B^{-2/b} \left(\frac{\pi^2}{6b^2} + \frac{1}{Zb^3} [a\pi^2/3 + (1-b)(\pi^2 v/3 - \psi''(1))] \right). \quad (12)$$

We have defined $v = (a/b) \ln Z + \gamma$, where $\gamma \approx 0.577$ is the Euler-Mascheroni constant, and $\psi''(1) \approx -2.404$ is the tetragamma function [46]. Despite increasing complexity of the calculation the leading term in the third and fourth central moments are given by simple expressions:

$$m_3 = B^{-3/b} Z^{3/b-3} \left(-\frac{\psi''(1)}{b^3} + \delta_3 \right), \quad (13)$$

$$m_4 = B^{-4/b} Z^{4/b-4} \left(\frac{3\pi^4}{20b^4} + \delta_4 \right). \quad (14)$$

The correction terms are of the order $\{\delta_3, \delta_4\} \propto Z^{-1}$. For example $\delta_3 = \frac{1}{60Zb^4} [90a\pi^2 v(v-1) - 11\pi^4(b-1) - 180\psi''(1)(a-v(b-1))]$ [23]. We are now in the position to compute skewness and kurtosis and thus find:

$$S = -m_3/m_2^{3/2} = 6^{3/2}\psi''(1)/\pi^3 + O(Z^{-1}), \quad (15)$$

$$K = m_4/m_2^2 = 27/5 + O(Z^{-1}), \quad (16)$$

which are central results of this section. Remarkably, to the leading order in $1/Z \ll 1$, both skewness and kurtosis are given by universal numbers $S \approx -1.139$ and $K \approx 5.4$, which are independent of the parameters of the system and are the same for both thermal and quantum phase slips. The magnitude of the correction terms δ_3, δ_4 is analyzed for different values of the ramp speed and different models of a weak link in [23].

Conclusion.—We have experimentally demonstrated the universality of higher moments – skewness and kurtosis – of the switching current distribution in superconducting nanocircuits. Our results are supported both by analytical modeling and by numerical simulations. We have also pointed out that the universality of higher moments is affected by extraneous noise [23] and suggested to use this observation to detect the presence of unwanted noise in the data.

The work was supported by DOE DE-FG02-07ER46453, ONR N000140910689, and NSF DMR 10-05645. V. V. was supported by the U.S. Department of Energy, Office of Basic Energy Sciences, Division of Materials Sciences and Engineering under Award DE-FG02-08ER46544 and by the Theoretical Interdisciplinary Physics and Astrophysics Center at JHU. A. L. acknowledges support from Michigan State University.

* Present address: Department of Microtechnology and Nanoscience (MC2), Chalmers University of Technology SE-412 96 Göteborg, Sweden, EU

- [1] A. A. Clerk *et al.*, Rev. Mod. Phys. **82**, 1155 (2010).
- [2] *Quantum Noise in Mesoscopic Physics*, Proceedings of the NATO Advanced Research Workshop edited by Yu. V. Nazarov (Springer, 2003).
- [3] B. Reulet, J. Senzier, and D. E. Prober, Phys. Rev. Lett. **91**, 196601 (2003).
- [4] For a review, see M. H. Devoret *et al.*, in *Quantum Tunneling in Condensed Media*, edited by Yu. Kagan and

- A. J. Leggett (Elsevier, 1992), p. 313, and references therein.
- [5] N. Giordano, Phys. Rev. Lett. **61**, **2137** (1988); Phys. Rev. Lett. **63**, **2417** (1989); Phys. Rev. B **41**, **6350** (1990).
 - [6] C. N. Lau *et al.*, Phys. Rev. Lett. **87**, 217003 (2001).
 - [7] M. Sahu *et al.*, Nat. Phys. **5**, 503 (2009).
 - [8] W. A. Little, Phys. Rev. **156**, 396 (1967).
 - [9] T. Aref *et al.*, Phys. Rev. B **86**, 024507 (2012).
 - [10] A. Bezryadin, *Superconductivity in Nanowires*, (Wiley-VCH, 2012).
 - [11] A. O. Caldeira and A. J. Leggett, Ann. Phys. (N.Y.) **149**, 374 (1983).
 - [12] H. Grabert and U. Weiss, Phys. Rev. Lett **54**, 1605 (1985).
 - [13] M. P. A. Fisher and A. T. Dorsey, Phys. Rev. Lett **54**, 1609 (1985).
 - [14] D. S. Golubev and A. D. Zaikin, Phys. Rev. B **64**, 014504 (2001); Phys. Rev. B **78**, 144502 (2008).
 - [15] K. Yu. Arutyunov, D. S. Golubev, and A. D. Zaikin, Phys. Rep. **464**, 1 (2008).
 - [16] A. Levchenko and A. Kamenev, Phys. Rev. B **76**, 094518 (2007).
 - [17] P. Li *et al.*, Phys. Rev. Lett. **107**, 137004 (2011).
 - [18] N. Shah, D. Pekker, and P. M. Goldbart, Phys. Rev. Lett. **101**, 207001 (2007).
 - [19] D. Pekker *et al.*, Phys. Rev. B **80**, 214525 (2009).
 - [20] J. Kurkijärvi, Phys. Rev. B **6**, 832 (1972).
 - [21] A. Bezryadin, C. N. Lau, and M. Tinkham, Nature **404**, 971 (2000).
 - [22] K. S. Novoselov, *et. al.*, Nature **438**, 197 (2005).
 - [23] See Supplemenatry Material for details.
 - [24] Gil-Ho Lee *et al.*, Phys. Rev. Lett. **107**, 146605 (2011).
 - [25] M. Tinkham, *Introduction to Superconductivity*, 2nd ed. (McGraw, NY, 1996).
 - [26] Note that for graphene device we have set $T_q = 0$ since no low-temperature saturation in the standard deviation of the switching current was observed on them.
 - [27] U. C. Coskun *et al.*, Phys. Rev. Lett **108**, 097003 (2012).
 - [28] The power exponent $\eta = 3/2$ is characteristic for the Kramers-type escape problem from the potential barrier discribed by the cubic parabola.
 - [29] A. D. Zaikin and G. F. Zharkov, Sov. J. Low Temp. Phys. **7**, 184 (1981).
 - [30] P. Dubos *et al.*, Phys. Rev. B **63**, 064502 (2001).
 - [31] A. Levchenko, A. Kamenev, and L. Glazman Phys. Rev. B **74**, 212509 (2006).
 - [32] M. Titov and C. W. J. Beenakker Phys. Rev. B **74**, 041401 (2006).
 - [33] H. B. Heersche *et al.*, Nature (London) **446**, 56 (2007).
 - [34] F. Miao *et al.*, Science **317**, 1530 (2007).
 - [35] X. Du, I. Skachko, and E. Y. Andrei, Phys. Rev. B **77**, 184507 (2008).
 - [36] C. M. Ojeda-Aristizabal *et al.*, Phys. Rev. B **79**, 165436 (2009).
 - [37] D. Jeong *et al.*, Phys. Rev. B **83**, 094503 (2011).
 - [38] I. V. Borzenets *et al.*, Phys. Rev. Lett. **107**, 137005 (2011).
 - [39] J. S. Langer and V. Ambegaokar, Phys. Rev. **164**, 498 (1967).
 - [40] D. E. McCumber and B. I. Halperin, Phys. Rev. B **1**, 1054 (1970).
 - [41] M. Tinkham *et al.*, Phys. Rev. B **68**, 134515 (2003).
 - [42] M. W. Brenner *et al.*, Phys. Rev. B **83**, 184503 (2011); Phys. Rev. B **85**, 224507 (2012).
 - [43] J. Bardeen, Rev. Mod. Phys. **34**, 667 (1962).
 - [44] Fitting curves for nanowire samples were made using the cubic potential model for U , but the value of κ was adjusted, up to 30% of the theoretical value, to achieve best-fits.
 - [45] A. Garg, Phys. Rev. B **51**, 15592 (1995).
 - [46] Notice that in expression (12) for σ^2 coefficient of $1/Z$ term in the brackets is different from that given by Eq. (8) of Ref. 45 which appears to be in error.

SUPPLEMENTARY MATERIAL

Expansion Coefficients $f_j(n, \ln Z)$

Introducing new variables $r = n/b$ and $v = (a/b) \ln Z + \gamma$, we find that expansion coefficients introduced in Eq. (10) of the main text are given by the following expressions:

$$f_1(n, \ln Z) = vr, \quad (1)$$

$$f_2(n, \ln Z) = \frac{a}{b}(v+1)r + \frac{r(r-1)}{2} \left(v^2 + \frac{\pi^2}{6} \right), \quad (2)$$

$$f_3(n, \ln Z) = -\frac{ar}{2b} \left(v^2 + \frac{1}{b} [2v(b-a) + 2b - 3a] + \frac{\pi^2}{6} \right) + \frac{ar(r-1)}{b} \left(v^2 + v + \frac{\pi^2}{6} \right) + \frac{r(r-1)(r-2)}{6} \left(v^3 + \frac{\pi^2 v}{2} - \psi''(1) \right), \quad (3)$$

$$f_4(n, \ln Z) = \frac{ar}{3b} \left(v^3 + \frac{\pi^2 v^2}{2} - \psi''(1) + \frac{3(2b-3a)}{2b} \left(v^2 + \frac{\pi^2}{6} \right) - \frac{3av(3b-a)}{b^2} + \frac{3(2b-a)}{b} (v^2 - \gamma + \gamma^2) \right) + \frac{r(r-1)}{2} \left(\frac{a^2}{b^2} \left((v+1)^2 + \frac{\pi^2}{6} \right) - \frac{a}{2b} \left(v^3 + \frac{\pi^2 v}{2} - \psi''(1) + \frac{2(b-a)}{b} \left(v^2 + \frac{\pi^2}{6} \right) + \frac{v(2b-3a)}{b} \right) \right) + \frac{ar(r-1)(r-2)}{2b} \left(v^3 + v^3 \frac{\pi^2 + 2}{2} - \psi''(1) + \frac{\pi^2}{6} \right) + \frac{r(r-1)(r-2)(r-3)}{24} \left(v^4 + \pi^2 v^2 - 4v\psi''(1) + \frac{3\pi^2}{20} \right). \quad (4)$$

Fitting Parameters

TABLE I: Fitting Parameters for nanowire samples

| Sample | Ω_0 ($10^{12} s^{-1}$) | $I_c(0)$ (μA) | T_c (K) | T_q (K) |
|--------|---------------------------------|----------------------|-----------|-----------|
| A | 0.8 | 11.02 | 5.70 | 0.784 |
| B | 0.16 | 12.01 | 5.48 | 0.781 |
| C | 0.32 | 13.27 | 5.00 | 0.814 |
| D | 0.16 | 9.38 | 5.09 | 0.87 |
| E | 0.16 | 4.25 | 3.24 | 0.521 |
| F | 0.02 | 5.46 | 4.57 | 0.711 |

TABLE II: Fitting Parameters for SGS junction sample 111s

| Gate Voltage (V_g) | Ω_0 ($10^9 s^{-1}$) | R_N (Ω) | T_c (K) | D (cm^2/s) |
|------------------------|------------------------------|--------------------|-----------|----------------|
| 1 | 1.5 | 138 | 7.2 | 51 |
| 3 | 1.5 | 88 | 7.2 | 54 |
| 5 | 0.2 | 72.5 | 7.2 | 57 |
| -1 | 0.6 | 210 | 7.2 | 48 |

Analysis of correction terms δ_3 and δ_4

For our results to be valid the ramp rate $|\dot{\epsilon}|$ must be small (otherwise the system will not be able to maintain an equilibrium from the initial state). The typical range of the sweep rates used in the experiments is $|\dot{\epsilon}| \sim (10^{-7} - 10^{-5}) s^{-1}$. At operating temperature $T \sim 0.3K$ the typical value of the escape frequency translates into the parameter

TABLE III: Parameters of the thermal and quantum escape rates for various degrees of Ohmic damping encoded by the quality factor Q of a junction. The table is compiled from previous studies of phase slip junction (PSJ) and Josephson junction (JJ) models [1–10]. U_0 stands for $U(I = 0, T)$.

| Escape | Damping | A | B | a | b |
|-------------|----------|---------------------------------|-------------------------|--------|-------|
| Thermal-JJ | Low | $18\Omega_0 U_0 / 5\pi Q T$ | U_0 / T | 1 | $3/2$ |
| Thermal-JJ | Moderate | $\Omega_0 / 2\pi$ | U_0 / T | $-1/4$ | $3/2$ |
| Thermal-JJ | High | $\Omega_0 Q / 2\pi$ | U_0 / T | 0 | $3/2$ |
| Thermal-PCJ | Moderate | $\sqrt{U_0 / T}$ | U_0 / T | $3/8$ | $5/4$ |
| Quantum | None | $\sqrt{216 U_0 \Omega_0 / \pi}$ | $36 U_0 / 5 \Omega_0$ | $5/8$ | $5/4$ |
| Quantum | High | $\sqrt{3 U_0 \Omega_0 / Q^7}$ | $3\pi U_0 / Q \Omega_0$ | 0 | 1 |

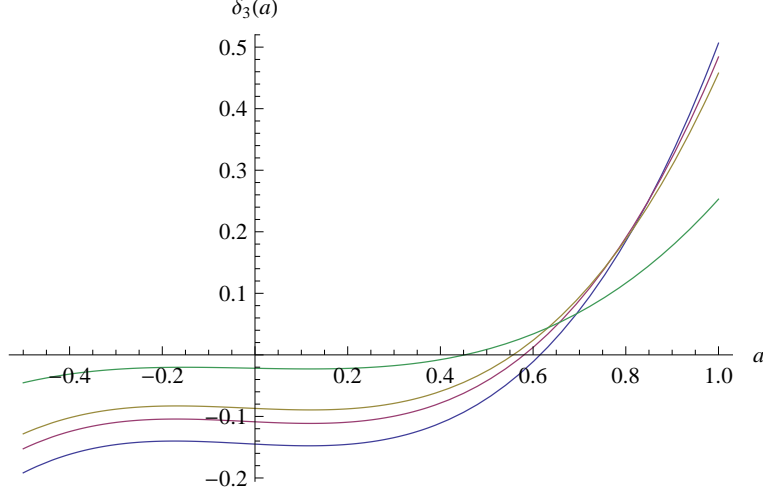


FIG. 1: Correction to skewness as a function of exponent a for different values of the ramp speed encoded by expansion parameter Z . $Z = 15, 20, 25, 100$ from the bottom to the top curve. Notice that for most models summarized in Table III parameter a falls in the range where δ_3 is nearly independent of a and is determined solely by the ramp speed. In particular, for PSJ model $a = 3/8$ and for JJ model $a = -1/4$.

$A \sim 10^{-12} \text{s}^{-1}$. For the critical current at that temperature we have $I_c \sim 10^{-5} \text{A}$ which translates into the parameter $B \sim 10^3$ that gives the scale for the height of the potential barrier for the escape. This together leads to an estimate of the expansion parameter $Z \sim 15$.

Now we present estimates that give some measure of the importance of correction terms δ_3 and δ_4 in our expressions for skewness and kurtosis versus power a and expansion parameter Z for the JJ model with $b = 3/2$. Given that theoretical calculations of the attempt frequency Ω (the pre-exponential factor in the escape rate) are quite challenging, the power-law exponent ν (or, in the reduced notation of Eq. 6 parameter a) is uncertain and is still a subject of debate. To the leading order the expression for δ_3 reads

$$\delta_3 = \frac{1}{60Zb^4} [90a\pi^2 v(v-1) - 11\pi^4(b-1) - 180\psi''(1)(a - v(b-1))]. \quad (5)$$

From Fig. 1 we conclude that the magnitude of δ_3 is about 10% of the universal value of S . The expression for δ_4 is implicit in Eq. (4) for $f_4(n, \ln Z)$ and also $f_5(n, \ln Z)$. Taking $a = 0$ for simplicity we find

$$\delta_4 = \frac{1-b}{5Zb^5} [3\gamma\pi^4 - 15\pi^2\psi''(1) - 10\psi^{(4)}(1)]. \quad (6)$$

For the value of Z estimated above ($Z \sim 15$) and for the JJ model with $b = 3/2$ one finds $\delta_4 \approx -0.679$ which changes K by about 10%. These estimates provide a firm assurance for the consistency of our results.

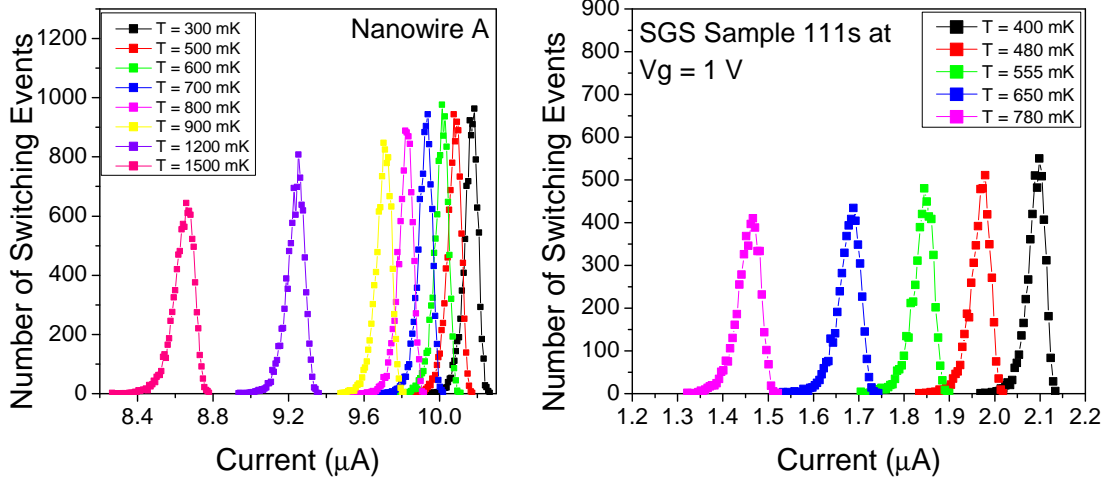


FIG. 2: Number of switching events versus current for superconducting nanowire A (left) and for superconductor-graphene-superconductor junction, Sample 111s, at a gate voltage of $V_g = 1$ V (right) plotted at various temperatures. To plot these distributions of the switching current the bin size was chosen 8.15 nA for the nanowire and 5 nA for graphene. Solid lines are given as guides to the eye. Note that the height of the distribution for the nanowire saturates below 0.7K, indicating that the switching is initiated by quantum phase slips at these low temperatures.

Switching current distribution

For completeness we provide several representative examples of phase-slip induced switching current distributions for both types of devices used in our experiments, see Fig. 2 for details.

Distribution moments for SGS sample 105.

Fig. 3 shows temperature dependence of first four moments of switching current distributions for SGS sample 105 - our second graphene sample. Each point is based on 10^4 measurements of the switching current. This junction has a much larger width (dimension across the current) $W = 214 \mu\text{m}$ and hence graphene area, but shows qualitatively the same behavior of higher moments as SGS sample 111s ($W = 9.9 \mu\text{m}$). Namely, the skewness is near -1 and the kurtosis is near 5, independently of temperature or gate voltage. Since the sample area is much larger, it is somewhat more sensitive to external perturbations. Namely, at temperatures below 350 mK some anomalous switching events occur at unexpectedly low bias current. Typically, out of 10^4 measured events, two or three switching events deviate significantly (by more than 10 standard deviations) from the general population of the switching distribution. Such anomalous events are very rare, and are believed to be unrelated to thermal (and/or quantum) fluctuations which we investigate here. Therefore we eliminate such points from our statistical analysis. They represent non-Gaussian extraneous perturbations of unknown origin. As stated above, no more than 2 or 3 anomalous points, out of 10^4 total, are excluded. Note that at temperatures greater than 350 mK no switching events have been excluded from the analysis because no such anomalously low-current switching events were observed at $T > 350$ mK. It is clear from Fig. 3 that the agreement with the model is reasonably good at all temperatures tested.

Numerical Simulations of Extraneous Noise

Although most samples produced switching distributions with $S \approx -1$ and $K \approx 5$, nanowire samples B and F and SGS sample 105 have slight, but noticeable deviations from these values. Such deviations pull the moments

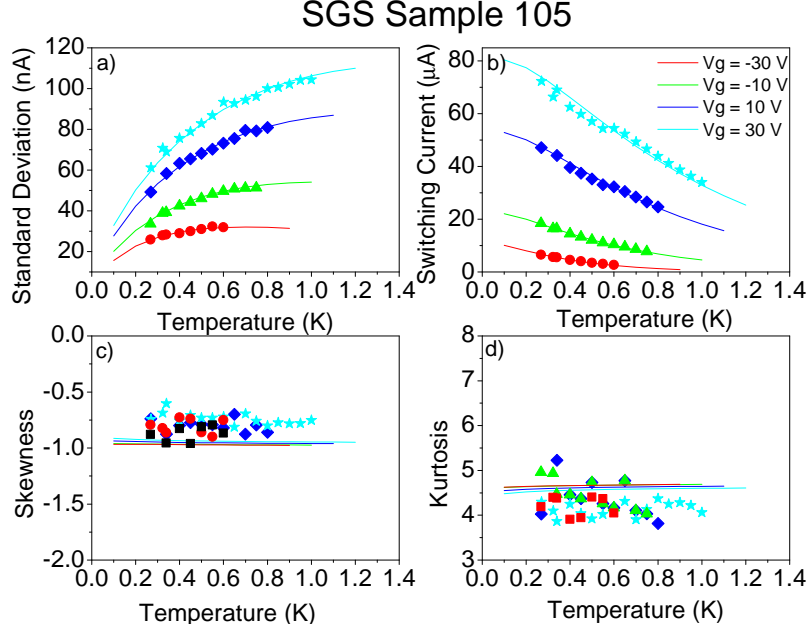


FIG. 3: Mean, standard deviation, skewness and kurtosis of switching current distribution for SGS sample 105. Symbols correspond to gate voltages as indicated on the legend in the top right corner. Solid lines are obtained through a fitting procedure analogous to that utilized for sample 111s with no extraneous noise. Fitting parameter R_N lies in the range $R_N \approx 2 - 10 \Omega$ while $D \approx 10 - 30 \text{ cm}^2/\text{s}$. These values are consistent with the geometry of this sample.

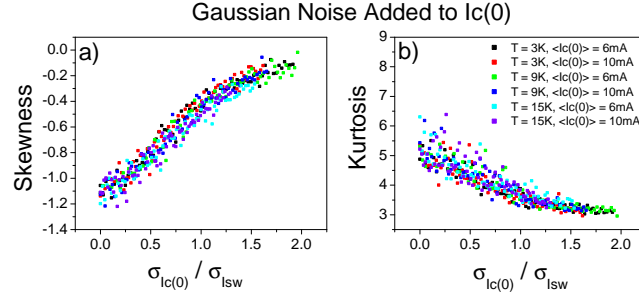


FIG. 4: Numerical modeling of the variation of the skewness (a) and kurtosis (b) in response to extraneous Gaussian noise of the critical current. The horizontal axis is the ratio of the standard deviation of the critical current of the wire $\sigma_{I_c(0)}$ and the standard deviation of the switching current $\sigma_{I_{SW}}$ which occurs if $I_c(0)$ does not fluctuate.

closer to those of a Gaussian distribution. We attribute such trend to white noise present within the system which could be caused by e.g. depairing current fluctuations brought about by time-dependent morphological changes of our amorphous wires. Utilizing the same numerical model as used to fit the curves in Figs. 1 and 2 in the main text, we examined how random noise in the critical current could affect the skewness and kurtosis of our nanowire samples. To do this, we allowed the critical current to vary about a mean value with Gaussian probability between the measurement runs. Results are shown in Fig. 4. We find that upon inclusion of such extraneous noise both skewness and kurtosis decrease in absolute values. Based on this observation we conjecture that reduction of the magnitude of higher moments from their universal values should be taken with caution and may signal about the presence of undesirable noise effects.

* Present address: Department of Microtechnology and Nanoscience (MC2), Chalmers University of Technology SE-412 96 Göteborg, Sweden, EU

[1] J. S. Langer and V. Ambegaokar, Phys. Rev. **164**, 498 (1967).

- [2] D. E. McCumber and B. I. Halperin, Phys. Rev. B **1**, 1054 (1970).
- [3] A. I. Larkin and Yu. N. Ovchinnikov, Zh. Eksp. Teor. Fiz. **86**, 719 (1984) [Sov. Phys. JETP **59**, 420 (1984)].
- [4] H. Grabert and U. Weiss, Phys. Rev. Lett **54**, 1605 (1985).
- [5] M. P. A. Fisher and A. T. Dorsey, Phys. Rev. Lett **54**, 1609 (1985).
- [6] P. Hanngi, P. Talkner and M. Borkovec, Rev. Mod. Phys. **62**, 251 (1990).
- [7] A. Garg, Phys. Rev. B **51**, 15592 (1995).
- [8] M. Tinkham *et al.*, Phys. Rev. B **68**, 134515 (2003).
- [9] D. S. Golubev and A. D. Zaikin, Phys. Rev. B **64**, 014504 (2001); Phys. Rev. B **78**, 144502 (2008).
- [10] K. Yu. Arutyunov, D. S. Golubev, and A. D. Zaikin, Phys. Rep. **464**, 1 (2008).